Chiroptical properties from time-dependent density functional theory. II. Optical rotations of small to medium size organic molecules

ARTICLE *in* THE JOURNAL OF CHEMICAL PHYSICS · JULY 2002

Impact Factor: 2.95 · DOI: 10.1063/1.1477925

Chiroptical properties from time-dependent density functional theory. II. Optical rotations of small to medium sized organic molecules

Jochen Autschbach,[a] Serguei Patchkovskii,[b] and Tom Ziegler[c]
Department of Chemistry, The University of Calgary, 2500 University Drive NW, Calgary, Alberta, T2N 1N4 Canada

Stan J. A. van Gisbergen
Scientific Computing and Modeling and Theoretical Chemistry, FEW, Vrije Universiteit, De Boelelaan 1083, 1081 HV Amsterdam, The Netherlands

Evert Jan Baerends
Theoretical Chemistry, FEW, Vrije Universiteit, De Boelelaan 1083, 1081 HV Amsterdam, The Netherlands

(Received 24 January 2002; accepted 22 March 2002)

We report an implementation for the computation of optical rotations within the Amsterdam Density Functional program package. The code is based on time-dependent density functional response theory. Optical rotations have been calculated for a test set of 36 organic molecules with various density functionals, and employing basis sets of different quality. The results obtained in this work with nonhybrid functionals are comparable in quality to those recently reported by other authors for the B3LYP hybrid functional, but show a somewhat larger tendency to produce outlyers. The median error is approximately $20°/(\mathrm{dm\,g/cm^3})$ for specific rotations $[\alpha]_D$ as compared to experimental data (approximately 30% median deviation from experimental values). Thereby it is demonstrated that density functional computations can be employed to assist with the solution of stereochemical problems in case the specific rotations of the species involved are not small and their structures are rigid. Recent newly developed functionals are investigated with respect to their applicability in computations of optical rotations. © *2002 American Institute of Physics.*
[DOI: 10.1063/1.1477925]

I. INTRODUCTION

Optical activity is of high importance in many fields of chemical and biochemical research.[1,2] The related experimental techniques such as circular dichroism (CD) spectroscopy[3] or the measurement of optical rotations (OR) and optical rotation dispersion (ORD)[4] are able to specifically distinguish between the optical antipodes of a chiral molecule that otherwise have the same physical properties. Theoretical methods that are able to assist the experimental research in this field are therefore of high importance.[5–8]

The currently most applied method in first-principles quantum chemical calculations is density functional theory (DFT) because it combines computational efficiency with often reliable accuracy of the results. Not surprisingly therefore, there has been recently an increasing interest in the computation of optical activity related observables by time-dependent density functional theory[9–11] (TDDFT). For example, TDDFT implementations for electronic circular dichroism have been presented by Furche *et al.*[12,13] in 2000 and by Autschbach *et al.*[14] in 2002. Vibrational circular dichroism (VCD) has already been implemented for DFT by Stephens *et al.* in 1996.[15,16] TDDFT implementations for the computation of frequency dependent optical rotations (ORs) into the GAUSSIAN and the TURBOMOLE program packages have been reported in 2001 by Stephens *et al.*[17] and by Grimme,[18] respectively. Both these works on ORs employed the well known B3LYP hybrid density functional (and Hartree–Fock in Ref. 17 for comparison with Ref. 8) and have been applied to a number of molecules. Very recently, B3LYP optical rotations have also been compared to data obtained from singles and doubles coupled cluster response theory, with promising results.[19] A numerical real-time approach applied to the OR and CD of methyloxirane and C_{70} based on the local density approximation (LDA) has been published in Ref. 20 but produced poor agreement with respect to experiment in the case of ORs. So far, no comprehensive OR study with ''pure'' density functionals [based on standard LDA or generalized gradient approximations (GGA)] is available. Further, there are newly developed functionals reported in the literature that have been shown to significantly improve computational results for response properties caused by external electric field perturbations. Therefore the question of their applicability to mixed electric/magnetic perturbations has to be addressed. In Refs. 17 and 18, the B3LYP functional has been shown to yield quite reliable results for small to medium sized organic molecules with rigid structures for which the specific rotations are not small $[\gtrsim 25°/(\mathrm{dm\,g/cm^3})]$, and therefore allows for routine applications for this type of systems. It is important

[a]Author to whom correspondence should be addressed; electronic mail: jautschb@ucalgary.ca
[b]Present address: Steacie Institute for Molecular Sciences, NRC, 100 Sussex Dr., Ottawa, Ontario K1A 0R6, Canada.
[c]Electronic mail: ziegler@chem.ucalgary.ca

to know how various "pure" density functionals perform in comparison.

It is our aim here to demonstrate that, provided the use of appropriate basis sets, it is possible to obtain optical rotations for organic molecules with nonhybrid density functionals that afford almost the same quality as the ones that are obtained with the B3LYP functional. For this purpose, we have selected the test set of 36 organic molecules shown in Fig. 1 and computed the optical rotation parameter at the sodium D line wavelength ($\lambda = 589.3$ nm). A new implementation for the computation of frequency dependent optical rotations has been developed within the Amsterdam Density Functional (ADF) program package[21–24] as an extension of its existing RESPONSE module[25,26] and applied to the molecules in Fig. 1. Either the electric or the magnetic field can be chosen as the perturbation from which the self-consistent first-order potential is computed. Results have been obtained with standard LDA and GGA functionals, with the statistical average of orbital Kohn–Sham potentials (SAOP),[27] and with our recently developed self-interaction corrected (SIC) density functional method.[28] The quality of the basis set is a critical issue. Our findings corroborate the results previously reported by other authors, namely that it is vital to incorporate diffuse functions in the basis set in order to achieve results with a relative median error of about 30% or less. However, because of the nature of the magnetic field perturbation, usage of additional polarization functions as compared to the "standard" polarized triple-ζ ADF Slater basis sets also significantly improves the computational results (in some cases even more than the use of diffuse functions instead). This suggests that significant improvement of the results might be still possible by merging the flexibility of both types of basis sets for future applications. Regarding the choice of density functionals we find that at the present stage no definite answer can be given as to which of the pure density functionals performs best on average.

In Sec. II we briefly summarize the underlying methodology for our implementation, and the computational details are listed in Sec. III. In Sec. IV, the computational data are reported and compared to experimental and other theoretical results. Finally, some concluding remarks and an outlook are given in Sec. V.

II. METHODOLOGY

The computation of optical rotations with the ADF program[21–24] has been realized as an extension of its existing RESPONSE module[25,26] that is capable of computing various frequency dependent electric polarizabilities. In Ref. 29 we have previously outlined a straightforward way of extending such a code in order to treat magnetic properties as well. A related discussion can be found, e.g., in Refs. 12 and 30. We will summarize the results here for convenience: In the sum-over-states (SOS) approach, the optical rotation parameter reads[6,31,32] (in dimensionless atomic units with $h = 2\pi$, $e = 1$, $4\pi\epsilon_0 = 1$, $m_e = 1$, and $c \approx 137.036$)

$$\beta(\omega) = \frac{2c}{3} \sum_{\lambda} \frac{\mathrm{Im}(\boldsymbol{\mu}_{0\lambda} \cdot \boldsymbol{m}_{\lambda 0})}{\omega_{0\lambda}^2 - \omega^2} = \frac{2c}{3} \sum_{\lambda} \frac{R_{0\lambda}}{\omega_{0\lambda}^2 - \omega^2}, \qquad (1)$$

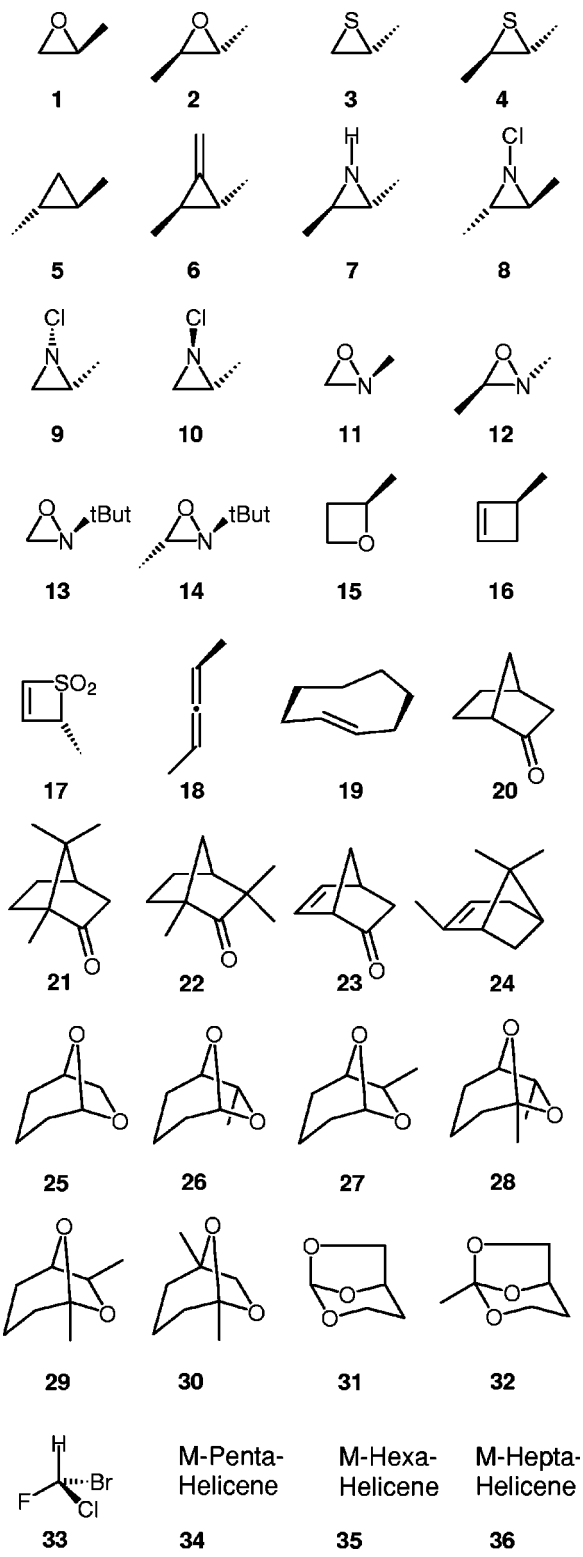

FIG. 1. The 36 molecules of the test set and their stereochemical configurations, for which computations have been carried out.

with ω being the frequency of the perturbing field, $\omega_{0\lambda}$ the excitation frequencies (= excitation energies in atomic units), and $\boldsymbol{\mu}_{0\lambda} = \langle \Psi_0 | \hat{\boldsymbol{\mu}} | \Psi_\lambda \rangle$ and $\boldsymbol{m}_{\lambda 0} = \langle \Psi_\lambda | \hat{\boldsymbol{m}} | \Psi_0 \rangle$ the electric and magnetic transition dipole moment vectors. The electric and magnetic dipole moment operators are $\hat{\boldsymbol{\mu}} = -e\boldsymbol{r}$ and $\hat{\boldsymbol{m}} = -(e/2m_e c)(\mathbf{r} \times \hat{\boldsymbol{p}})$, respectively. The terms $R_{0\lambda}$ are the rotatory strengths for the excitations $0 \rightarrow \lambda$ and represent the

integrated intensities of individual bands in the CD spectrum. Here, 0 and λ denote the electronic ground state and one of the excited electronic states of the molecule under investigation. The expression (1) arises from considering a perturbation $\boldsymbol{\mu}'(\omega)$ of the electric dipole moment by a time dependent magnetic dipole field, or likewise by the perturbation $\boldsymbol{m}'(\omega)$ of the magnetic dipole moment by an electric dipole field, and by using all the field free eigenfunctions Ψ_λ as a complete basis set in which the perturbed wave function is expanded. Within a density-matrix based TDDFT approach, $\boldsymbol{\mu}'(\omega)$ and $\boldsymbol{m}'(\omega)$ are directly expressed based on perturbations of the electron density or the current density by a magnetic or electric field, respectively, as

$$\mu'(\omega)=\sum_{(ai\sigma)} D_{ai\sigma}(X_{ai\sigma}+Y_{ai\sigma})=\boldsymbol{D}\cdot(\boldsymbol{X}+\boldsymbol{Y}), \tag{2a}$$

$$m'(\omega)=\sum_{(ai\sigma)} M_{ai\sigma}(X_{ai\sigma}-Y_{ai\sigma})=\boldsymbol{M}\cdot(\boldsymbol{X}-\boldsymbol{Y}). \tag{2b}$$

Here, $\boldsymbol{M}$ and $\boldsymbol{D}$ are vectors containing all the matrix elements $D_{ai\sigma}$ and $M_{ai\sigma}$ of $\hat{\boldsymbol{\mu}}$ and $-\hat{\boldsymbol{m}}$, respectively, involving ordered occupied (i)–virtual (a) real Kohn–Sham spin (σ) orbitals pairs, and a single composite index ($ai\sigma$). [Please note that some of the expressions in Ref. 29 contain a sign error due to an inverted sign in Eq. (2b)]. We assume orbitals occupations of 0 and 1. The frequency dependent response of the density or current density is related to the $\boldsymbol{X}$ and $\boldsymbol{Y}$ density matrix elements. Note that $Y_{ai\sigma}=X_{ia\sigma}$.

Considering the matrix elements $V_{ai\sigma}$ and $W_{ai\sigma}=V_{ia\sigma}$ of the external perturbation in a similar vector notation $\boldsymbol{V},\boldsymbol{W}$, the following equation system can be derived for X and Y:

$$(\mathsf{A}+\mathsf{B})(\boldsymbol{X}+\boldsymbol{Y})+\omega\mathsf{C}(\boldsymbol{Y}-\boldsymbol{X})=\boldsymbol{V}+\boldsymbol{W}, \tag{3a}$$

$$(\mathsf{A}-\mathsf{B})(\boldsymbol{Y}-\boldsymbol{X})+\omega\mathsf{C}(\boldsymbol{X}+\boldsymbol{Y})=\boldsymbol{W}-\boldsymbol{V}. \tag{3b}$$

Here, the symbols A, B, and C denote matrices based on the indices ($ai\sigma$) and ($bj\tau$). We will not repeat the explicit expressions for them but refer to the literature instead.[29,33–35] Is is important to stress, though, that A and B are related to the first-order response of the system to an external perturbation and represent the actual computational problem to be solved (apart from obtaining an accurate unperturbed set of Kohn–Sham orbitals and energies). Also, approximate expressions for the DFT specific exchange-correlation (XC) part of the first-order Kohn–Sham potential enter the expressions for A and B. Generally, A and B have to be thought of as frequency dependent quantities, but in actual molecular computations, often a frequency independent local-density approximation [adiabatic local density approximation (ALDA)] is used.[13,25] C is related to the orbital occupations and just equals the negative unit matrix here.

In order to compute the optical rotation parameter, one consequently needs to obtain expressions for $(\boldsymbol{X}+\boldsymbol{Y})$ or $(\boldsymbol{X}-\boldsymbol{Y})$ in Eqs. (2a) and (2b). For perturbations with $\boldsymbol{V}=\boldsymbol{W}$ such as an electric field, the following equation for $(\boldsymbol{X}+\boldsymbol{Y})$ is derived from Eq. (3):

$$[(\mathsf{A}+\mathsf{B})+\omega^2\mathsf{S}](\boldsymbol{X}+\boldsymbol{Y})=2\boldsymbol{V}. \tag{4}$$

The matrix $\mathsf{S}=-\mathsf{C}(\mathsf{A}-\mathsf{B})^{-1}\mathsf{C}$ is diagonal and has the components $(\epsilon_{a\sigma}-\epsilon_{i\sigma})^{-1}$, with the ϵ's being the unperturbed (i.e., field free) Kohn–Sham orbital energies. The solution of this equation is used in the existing RESPONSE implementation of the ADF program to compute, e.g., dipole polarizabilities. Due to the large dimensions of the matrices A and B, their computation and storage is not practicable for all but the smallest molecules and basis sets. Therefore the equation system (4) is in practice solved iteratively in such a way that the matrix on its left-hand side is never explicitly computed. The technical details, also with respect to the implementation of ''linear scaling'' techniques, are extensively described in Refs. 26 and 36.

Upon substitution of $(\boldsymbol{X}+\boldsymbol{Y})$ in Eq. (3b) a solution for $(\boldsymbol{X}-\boldsymbol{Y})$ in an electric dipole field can be obtained, and from this the optical rotation parameter $\beta(\omega)$. In practice, this is simply achieved by multiplication of the converged intermediate result for $(\boldsymbol{X}+\boldsymbol{Y})$ during an ADF dipole polarizability computation by $(2c/3)\boldsymbol{M}\mathsf{C}^{-1}\mathsf{S}$. This extension involves only minor changes of the existing code, as already outlined in Ref. 29, since the required integrals of the magnetic moment operator over the Kohn–Sham molecular orbitals are already available from the recent CD implementation.[14] Formally,[29] this procedure leads to the final expression for the optical rotation parameter:

$$\beta(\omega)=-\frac{2c}{3}\mathrm{Im}(\boldsymbol{M}\mathsf{C}^{-1}\mathsf{S}^{1/2}[\omega^2-\Omega]^{-1}\mathsf{S}^{-1/2}\boldsymbol{D}). \tag{5}$$

Here, $\Omega=-\mathsf{S}^{-1/2}(\mathsf{A}+\mathsf{B})\mathsf{S}^{-1/2}$ is a Hermitian matrix. By transforming $[\omega^2-\Omega]^{-1}$ in Eq. (5) into the basis of the eigenvectors of Ω with ''eigenvalues'' $\omega_{0\lambda}^2$, the TDDFT analog of the sum-over-states formula (1) for $\beta(\omega)$ is obtained.[29,34] From this, TDDFT expressions for $\boldsymbol{\mu}_{0\lambda}$ and $\boldsymbol{m}_{0\lambda}$ can be extracted. We have previously extended the RESPONSE module of the ADF program for the computation of rotatory strengths based on these expressions, which allows for the simulation of electronic CD spectra of molecules.[14] A similar approach has been published earlier in Ref. 12.

Another possibile way in which to compute $\beta(\omega)$ is to solve directly for $(\boldsymbol{X}+\boldsymbol{Y})$ in the presence of a magnetic field. For such a case where $\boldsymbol{V}=-\boldsymbol{W}$, the resulting equation system, derived from Eqs. (3), is

$$[\mathsf{S}^{-1}(\mathsf{A}+\mathsf{B})+\omega^2](\boldsymbol{X}+\boldsymbol{Y})=-2\omega\mathsf{C}^{-1}\boldsymbol{V}. \tag{6}$$

This can be recast into the form of Eq. (4), and therefore the existing RESPONSE code implementation for dipole polarizabilities can be utilized for its solution, by noting that Eq. (6) can be rewritten as

$$[(\mathsf{A}+\mathsf{B})+\omega^2\mathsf{S}](\tilde{\boldsymbol{X}}+\tilde{\boldsymbol{Y}})=2\tilde{\boldsymbol{V}} \tag{7}$$

with $\tilde{\boldsymbol{V}}=-\mathsf{S}\mathsf{C}^{-1}\boldsymbol{V}$ and $(\tilde{\boldsymbol{X}}+\tilde{\boldsymbol{Y}})=(\boldsymbol{X}+\boldsymbol{Y})/\omega$. This means that, by using $\tilde{\boldsymbol{V}}$ for the matrix elements of a perturbing magnetic field in Eq. (4), one solves effectively for $(\boldsymbol{X}+\boldsymbol{Y})/\omega$ which is directly related to the optical rotation parameter in case the matrix elements $\boldsymbol{V}$ are due to an external magnetic dipole field. The final formal expression for $\beta(\omega)$ obtained from this approach is the same as Eq. (5). Since the availability of $(\boldsymbol{X}+\boldsymbol{Y})$ in the presence of a magnetic field gives in turn access to $(\boldsymbol{X}-\boldsymbol{Y})$ through the equation system (3), this also opens a way for the computation of magnetiza-

tions due to time-dependent magnetic dipole fields (with some limitations that are discussed in Ref. 29).

We have implemented both alternatives for the computation of $\beta(\omega)$ that are outlined above. Ideally, both methods should yield the same results. However, in practical ADF computations this accuracy cannot be achieved for various technical reasons (numerical integration accuracy, fit of the electron density for the computation of the Coulomb potential, numerical sensitivity of the results, etc.). We have found in our computations that the results obtained from either the electric field or the magnetic field perturbation typically agree to within approximately 1%. This can be used as an indication of the numerical quality of the result. See also the next paragraph. All final results that are presented in Sec. IV have been obtained by choosing the electric field as the external perturbation.

Generally, we have found that the computation of $\beta(\omega)$ from Eq. (5) is a numerically rather delicate problem, and consequently tight convergence criteria for the SCF cycle and for the determination of the first-order Kohn–Sham potential as well as a high numerical integration accuracy are required. Typically, the optical rotation tensor, from which β is evaluated as its trace, has large individual elements on its diagonal that almost cancel each other. The small remaining difference represents the optical rotation parameter which is compared to experimental data. For this reason, the numerical accuracy for optical rotations is not as favorable as, say, for dipole polarizabilities. In two cases, the convergence behavior of the SIC functional did not yield an accurate enough zeroth order solution in order to determine reliable optical rotations. The results reported in Sec. IV can be expected to be numerically accurate to about three digits for typical cases. A similar accuracy has been reported in Ref. 18 for an alternative implementation of TDDFT optical rotations.

Currently we do not account for the gauge dependence of the results by the use of a field dependent basis set (such as GIAOs). Contradictory statements can be found in the literature whether it is mandatory[17] or not[8,18] to enforce the gauge-independence of chiroptical properties, which seems to be partially motivated by the availability or nonavailability of a respective code implementation. Very recently, it has been shown that, provided use is made of high quality basis sets including diffuse functions, physically meaningful results can be obtained for optical rotations without explicitly enforcing the gauge invariance.[18] Likewise, we have recently demonstrated that in the case of the computation of rotatory strengths the gauge dependence of the results is only very minor in case high quality basis sets including diffuse functions were employed.[14] Comparison with experimental data clearly indicates that reliable results for chiroptical properties are only obtained with such high quality basis sets in which case the gauge dependence is not very pronounced. The computation of chiroptical observables, given as total molecular properties, is very much unlike the case of NMR chemical shifts where extremely sensitive gauge dependent properties of different atoms within a molecule are evaluated and for which a gauge independent formalism is therefore vital. Problematic cases for optical rotations could be large molecules for which the optical rotations are dominantly caused by a small, localized chromophor that is located far from the center of mass of the molecule.

TABLE I. Basis sets that have been used for the computations. The number of s, p, d, and f Slater functions for the valence shell of p-block elements and the number of polarization and diffuse functions are listed in order to illustrate the flexibility of the basis sets. Number of basis functions for hydrogen in parentheses.

Basis	Valence shell	Polarization	Diffuse	Reference
III	$2s$, $2p$	$1d$		21
	($2s$)	($1p$)		
IV	$3s$, $3p$	$1d$		21
	($3s$)	($1p$)		
Vd	$3s$, $3p$	$1d$,$1f$	$1s$, $1p$, $1d$	21, 25, 37, 38
	($3s$)	($1p$,$1d$)	($2p$)	
Vp	$3s$, $3p$	$2d$, $2f$		28
	($3s$)	($3p$,$2d$)		

III. COMPUTATIONAL DETAILS

Computations of frequency dependent optical rotations have been carried out with a modified version of the Amsterdam Density Functional program (ADF).[21–24] The basis sets that have been used are the Slater type basis sets that are part of the ADF package[21] and are described in Table I. The roman numbering "I...V" refers to the ADF basis set database.[21] The basis Vd has been confirmed to yield reliable excitation energies and electric response properties,[37,38] and has also been successfully applied by us to the simulation of CD spectra of organic molecules.[14] Due to the lack of a Vd basis for S, Cl, and Br, we have employed a recently developed all-electron even tempered basis including diffuse functions[39] together with the Vd basis for H, C, N, O, and F in the case of molecules containing these elements ($9s$, $7p$, $4d$, and $2f$ functions for S and Cl, and $11s$, $9p$, $7d$, and $2f$ for Br). We have previously found that this even-tempered basis yields very similar results to Vd for H–C–N–O–F compounds and should therefore also be of comparable quality for the heavier elements. Each basis is accompanied by an auxiliary fit set in which the electron density is represented and used to evaluate the Coulomb potential in an efficient way. The basis Vp has been used recently by us in a study of NMR chemical shifts[28] and can therefore be expected to yield improvements over basis IV for other magnetic properties as well. It is accompanied with auxiliary fit sets that have been optimized for the use with our new implementation of a self-interaction corrected (SIC) functional (see below). We refer to Ref. 28 for details regarding the Vp basis set.

As already mentioned, A and B in Eq. (3) are based upon the ALDA XC kernel in all computations. It has been demonstrated previously that this appears to be a rather good approximation for molecular response properties,[13,38,40] at least for those that are dominated by contributions from the low energy range of the electronic excitation spectrum. At the same time, approximations to the zeroth order Kohn–Sham potential, on which the unperturbed orbitals and orbital energies depend, significantly affect the results. Here we have evaluated four different functionals for the zeroth order

TABLE II. Specific rotations $[\alpha]_D$ for the molecules listed in Fig. 1. $[\alpha]_D$ values are given in the usual units of degree/(dm g/cm^3).

	Molecule, expt.$[\alpha]_D$[c,d]	Other DFT	This work[e] Method	This work[e] $[\alpha]_D$		Molecule, expt.$[\alpha]_D$[c,d]	Other DFT	This work[e] Method	This work[e] $[\alpha]_D$
1		−17.5[a]	LDA/IV	−89.4	**9**		78.5[a]	LDA/IV	111.4
		−13.8[b]	LDA/Vp	−1.2				LDA/Vp	141.6
	−18.7		LDA/Vd	−0.8		78.2		LDA/Vd	154.9
			GGA/IV	−88.8				GGA/IV	113.2
			GGA/Vp	−5.9				GGA/Vp	136.9
			GGA/Vd	−4.9				GGA/Vd	143.5
			SAOP/Vd	−1.2				SAOP/Vd	138.6
			SIC/Vp	−11.7				SIC/Vp	138.5
2		78.6[a]	LDA/IV	262.7	**10**		−133.2[a]	LDA/IV	−122.6
		72.7[b]	LDA/Vp	68.0				LDA/Vp	−91.0
	58.8		LDA/Vd	65.5		−103.4		LDA/Vd	−115.9
			GGA/IV	243.9				GGA/IV	−117.6
			GGA/Vp	68.0				GGA/Vp	−83.8
			GGA/Vd	75.6				GGA/Vd	−112.0
			SAOP/Vd	51.7				SAOP/Vd	−95.6
			SIC/Vp	63.9				SIC/Vp	−90.7
3		53.1[a]	LDA/IV	76.9	**11**		−128.6[a]	LDA/IV	−117.8
		63.6[b]	LDA/Vp	12.8				LDA/Vp	−118.1
	51.2		LDA/Vd	10.9				LDA/Vd	−114.3
			GGA/IV	74.2				GGA/IV	−108.7
			GGA/Vp	12.5				GGA/Vp	−108.7
			GGA/Vd	11.4				GGA/Vd	−105.7
			SAOP/Vd	13.7				SAOP/Vd	−61.1
			SIC/VP	75.8				SIC/Vp	−89.6
4		167.1[a]	LDA/IV	310.4	**12**		193.2[a]	LDA/IV	260.7
		177.1[b]	LDA/Vp	147.6				LDA/Vp	205.1
	129.0		LDA/Vd	125.0				LDA/Vd	201.2
			GGA/IV	277.5				GGA/IV	236.6
			GGA/Vp	129.2				GGA/Vp	186.0
			GGA/Vd	109.9				GGA/Vd	185.2
			SAOP/Vd	123.4				SAOP/Vd	134.6
			SIC/Vp	175.0				SIC/Vp	156.3
5		−59.0[a]	LDA/IV	−133.0	**13**		−16.3[a]	LDA/IV	59.2
		−54.7[b]	LDA/Vp	−50.4			−19.8[b]	LDA/Vp	8.9
	−42.0		LDA/Vd	−56.8		−34.5		LDA/Vd	30.1
			GGA/IV	−121.8				GGA/IV	43.3
			GGA/Vp	−51.4				GGA/Vp	1.7
			GGA/Vd	−67.0				GGA/Vd	20.9
			SAOP/Vd	−65.9				SAOP/Vd	45.3
			SIC/Vp	−60.3				SIC/Vp	−21.5
6		3.4[a]	LDA/IV	183.4	**14**		−86.0[a]	LDA/IV	−63.3
			LDA/Vp	39.8				LDA/Vp	−77.8
	57.6		LDA/Vd	23.1		−37.1		LDA/Vd	−63.4
			GGA/IV	127.1				GGA/IV	−65.5
			GGA/Vp	−12.2				GGA/Vp	−76.0
			GGA/Vd	−12.7				GGA/Vd	−66.0
			SAOP/Vd	−60.8				SAOP/Vd	−32.9
			SIC/Vp	−43.9				SIC/Vp	−88.2
7		103.1[a]	LDA/IV	279.8	**15**		−73.7[b]	LDA/IV	−53.4
		104.8[b]	LDA/Vp	110.3				LDA/Vp	−107.2
	103.8		LDA/Vd	106.6		−34.0		LDA/Vd	−115.8
			GGA/IV	256.4				GGA/IV	−29.4
			GGA/Vp	105.0				GGA/Vp	−81.3
			GGA/Vd	113.0				GGA/Vd	−92.9
			SAOP/Vd	98.6				SAOP/Vd	−62.9
			SIC/Vp	81.5				SIC/Vp	−40.5
8		−28.4[a]	LDA/IV	68.0	**16**		−171.7[a]	LDA/IV	−252.3
			LDA/Vp	−29.6			−153.2[b]	LDA/Vp	−183.1
	−16.8		LDA/Vd	−21.7		−176.0		LDA/Vd	−193.4
			GGA/IV	59.3				GGA/IV	−233.8
			GGA/Vp	−30.3				GGA/Vp	−168.9
			GGA/Vd	−19.5				GGA/Vd	−184.3
			SAOP/Vd	−28.0				SAOP/Vd	−174.9
			SIC/Vp	n.c.				SIC/Vp	−143.0

TABLE II. (*Continued*.)

Molecule, expt.$[\alpha]_D$[c,d]	Other DFT	This work[e] Method	This work[e] $[\alpha]_D$	Molecule, expt.$[\alpha]_D$[c,d]	Other DFT	This work[e] Method	This work[e] $[\alpha]_D$
17	−46.0[a]	LDA/IV	−29.3	**25**	94.2[a]	LDA/IV	116.4
		LDA/Vp	−41.9			LDA/Vp	105.3
−21.2		LDA/Vd	−27.1	115.0		LDA/Vd	103.2
		GGA/IV	−33.7			GGA/IV	112.0
		GGA/Vp	−43.7			GGA/Vp	103.2
		GGA/Vd	−27.9			GGA/Vd	100.0
		SAOP/Vd	−40.6			SAOP/Vd	98.1
		SIC/Vp	−27.1			SIC/Vp	88.0
18	135.4[a]	LDA/IV	161.1	**26**	118.3[a]	LDA/IV	141.0
	105.3[b]	LDA/Vp	182.1			LDA/Vp	154.9
81.0		LDA/Vd	194.6	108.1		LDA/Vd	134.9
(227)		GGA/IV	160.4			GGA/IV	125.9
		GGA/Vp	180.6			GGA/Vp	140.0
		GGA/Vd	189.3			GGA/Vd	121.1
		SAOP/Vd	203.2			SAOP/Vd	106.3
		SIC/Vp	181.3			SIC/Vp	91.5
19	417.0[b]	LDA/IV	339.7	**27**	83.1[a]	LDA/IV	114.5
		LDA/Vp	395.9			LDA/Vp	88.4
430.0		LDA/Vd	371.6	94.4		LDA/Vd	50.7
		GGA/IV	281.4			GGA/IV	112.9
		GGA/Vp	334.9			GGA/Vp	92.5
		GGA/Vd	309.5			GGA/Vd	45.6
		SAOP/Vd	280.7			SAOP/Vd	76.3
		SIC/Vp	294.2			SIC/Vp	97.2
20	20.3[b]	LDA/IV	42.7	**28**	80.9[a]	LDA/IV	79.3
		LDA/Vp	28.3			LDA/Vp	101.7
29.0		LDA/Vd	24.9	86.5		LDA/Vd	94.2
		GGA/IV	31.5			GGA/IV	75.2
		GGA/Vp	19.5			GGA/Vp	95.2
		GGA/Vd	17.3			GGA/Vd	79.6
		SAOP/Vd	−3.4			SAOP/Vd	95.7
		SIC/Vp	−16.9			SIC/Vp	72.9
21	60.7[a]	LDA/IV	98.8	**29**	42.9[a]	LDA/IV	56.7
	61.3[b]	LDA/Vp	101.6			LDA/Vp	35.4
44.1		LDA/Vd	100.9	66.3		LDA/Vd	22.0
		GGA/IV	85.5			GGA/IV	62.9
		GGA/Vp	89.6			GGA/Vp	43.1
		GGA/Vd	90.9			GGA/Vd	21.3
		SAOP/Vd	67.7			SAOP/Vd	62.3
		SIC/Vp	41.7			SIC/Vp	57.8
22	−67.4[a]	LDA/IV	−73.0	**30**	28.4[a]	LDA/IV	37.6
	−52.7[b]	LDA/Vp	−75.7			LDA/Vp	29.4
−50.5		LDA/Vd	−85.4	56.9		LDA/Vd	40.9
		GGA/IV	−69.2			GGA/IV	39.2
		GGA/Vp	−69.9			GGA/Vp	34.2
		GGA/Vd	−93.0			GGA/Vd	46.7
		SAOP/Vd	−82.5			SAOP/Vd	38.9
		SIC/Vp	−57.4			SIC/Vp	37.1
23	−1215.8[a]	LDA/IV	−1843.5	**31**	149.0[a]	LDA/IV	221.0
		LDA/Vp	−1850.9			LDA/Vp	193.0
−1146.0		LDA/Vd	−1861.9	175.8		LDA/Vd	203.3
		GGA/IV	−1663.7			GGA/IV	206.4
		GGA/Vp	−1684.3			GGA/Vp	180.8
		GGA/Vd	−1663.0			GGA/Vd	160.7
		SAOP/Vd	−1387.3			SAOP/Vd	153.6
		SIC/Vp	−1034.1			SIC/Vp	125.7
24	41.9[a]	LDA/IV	38.7	**32**	110.8[a]	LDA/IV	178.6
		LDA/Vp	38.4			LDA/Vp	142.0
51.6		LDA/Vd	46.1	139.2		LDA/Vd	164.8
		GGA/IV	44.9			GGA/IV	167.3
		GGA/Vp	45.1			GGA/Vp	133.7
		GGA/Vd	59.3			GGA/Vd	162.7
		SAOP/Vd	83.4			SAOP/Vd	124.5
		SIC/Vp	63.0			SIC/Vp	90.2

TABLE II. (*Continued*.)

Molecule, expt.$[\alpha]_D$[c,d]	Other DFT	This work[e] Method	This work[e] $[\alpha]_D$	Molecule, expt.$[\alpha]_D$[c,d]	Other DFT	This work[e] Method	This work[e] $[\alpha]_D$
33	3.7[b]	LDA/IV	3.5	**35**	−4887.0[b]	LDA/III	−5051.3
		LDA/Vp	3.7			LDA/IV	−5307.5
1.8		LDA/Vd	1.8	−3640.0		GGA/III	−5049.8
		GGA/IV	4.0			GGA/IV	−5258.8
		GGA/Vp	3.2			SAOP/III	−5343.2
		GGA/Vd	1.7	**36**		LDA/III	−7638.5
		SAOP/Vd	1.3			LDA/IV	−8486.8
		SIC/Vp	n.c.	−6200.0		GGA/III	−8164.3
34		LDA/III	−2993.5			GGA/IV	−8292.6
		LDA/IV	−3007.5			SAOP/III	−7691.1
−2160.0		GGA/III	−2993.3				
		GGA/IV	−2984.6				
		SAOP/III	−3051.8				

[a]Reference 17.
[b]Reference 18.
[c]See Fig. 1.
[d]Experimental values taken from the compilations in Refs. 17 and 18 except for **34** (Ref. 48) and **36** (Refs. 49 and 50). In some cases, the experimental value has been measured for the optical antipode and is consequently multiplied by −1.
[e]See Sec. III. "n.c." indicates insufficient SIC convergence in order to allow for a calculation of $[\alpha]_D$.

potential: the local density approximation (LDA) in the form of the Vosko–Wilk–Nusair[41] (VWN) functional, VWN + gradient corrections (GGA) in the form of the widely used Becke88-Perdew86 (BP86) functional,[42–44] and further the "statistical average of orbital potentials" (SAOP) by Schipper *et al.*[27] and the ADF implementation of the self-interaction corrected BP86 functional (SIC-BP68 or SIC) by Patchkovskii *et al.*[28] SAOP has been developed specifically with improvements of excitation energies and frequency dependent response properties in mind and it can therefore in principle be expected to yield some improvement over the VWN or BP86 functionals also for the optical rotations. We have previously found that SAOP yields improved results for individual rotatory strengths of selected molecules.[14] The SIC functional has been successfully applied by us[28] to NMR chemical shifts (and, somewhat less satisfactory, to nuclear spin-spin coupling constants). Therefore we might expect it to offer some improvements in the case of optical rotations as well, at least in some difficult cases, since they also represent a perturbation caused by an external magnetic field. As compared to more standard density functionals, application of the SIC functional requires the evaluation of the Coulomb potential due to individual orbital densities instead of just the total density. This requires a much more flexible auxiliary fit basis and thus we have carried out SIC computations only with the basis Vp for which an appropriate fit set has been previously generated.[28] We refer the reader to the literature[28] for details about the SIC functional and advantages and shortcomings that are associated with it. Mainly because of the necessary determination of the Coulomb potential for orbital densities, the computational expense for our SIC implementation is higher than for standard DFT, and therefore SIC has not been applied to the helicenes. For these molecules, we have further omitted computations with the basis set Vd. For our previous work[14] we have computed the CD spectrum of hexahelicene with both the IV and Vd bases and could not observe any significant differences. The helicenes have very intense low lying CD transitions that dominate also their optical rotations. It has already been shown in Ref. 18 that inclusion of diffuse functions has a negligible effect on the computed optical rotations of various helicenes. In order to illustrate the basis set dependence of their optical rotations, we have carried out computations for the helicenes with the basis sets III and IV instead.

For methyloxirane, dimethyloxirane, and the helicenes (see Fig. 1), previously reported Hartree–Fock optimized geometries were taken from Refs. 12 and 45 in order to be consistent with our previous work[14] and other investigations.[12] For other molecules that we have previously studied in Ref. 14, the same computationally optimized structures have been used in this work. Also for reasons of consistency with other work, the remaining molecules were optimized at the B3LYP/6-311G** level. For the computation of optical rotations we have employed center-of mass coordinates, where the Cartesian axes are aligned with the principal axes of inertia of the molecule. Optical rotation parameters $\beta(\omega)$ were calculated at the sodium D line frequency ($\lambda = 589.3$ nm) and converted to specific rotations $[\alpha]_D$ using standard molecular weights (based on isotope averaged atomic masses). Experimentally observed specific rotations $[\alpha]_\omega$ for the frequency ω in units of deg/(dm g/cm^3) are related to the optical rotation parameter $\beta(\omega)$ by[5,6]

$$[\alpha]_\omega = 7200 \frac{\omega^2 N_A}{c^2 M} \beta(\omega) \tag{8}$$

in the Gaussian system of units. $\beta(\omega)$ is here in units of cm^4, N_A is Avogadro's number, c is the speed of light in cm/s, and M is the molecular weight in g/mol. ω is the "circular" frequency of the perturbing field, related to its wavelength λ by $\lambda = (2\pi c)/\omega$. We initially compute $\beta(\omega)$ in atomic units. This leads to a conversion factor of about $38\,652/(M \text{ mol/g})$

from $\beta(D)$ in a.u. to $[\alpha]_D$ in deg/(dm g/cm^3). As in Ref. 18, the reported specific rotations do not contain the Lorentz factor of $(n^2+2)/3$ due to the solvent, with n being the solvent's refractive index. As can be seen from Fig. 2 our results over- or underestimate the experimentally observed values with approximately equal probability and therefore a rather ''balanced'' result is already obtained without considering the solvent influence via the Lorentz factor (the inclusion of which would consequently lead to a biased overall result[17]). This can likely be attributed to a compensation of errors, and more detailed studies are clearly needed in the future in order to clarify the effect of the solvent on the optical rotations.

Timings of the ADF RESPONSE module have been reported in detail in Ref. 36. In this work we have not yet employed the ''linear scaling'' features of the code described in this reference. There are no restrictions in the code that would prevent their usage, however, extensive benchmark calculations have yet to confirm that the results for the rather numerically sensitive optical rotations are not more strongly affected by these features than polarizabilities. Generally, the computation of the $\boldsymbol{D}$ and $\boldsymbol{M}$ matrix elements is a minor task as compared to the solution of Eq. (7), therefore the timings for the optical rotation computations are very similar to the ones reported in Ref. 36 for dipole polarizabilities.

IV. RESULTS AND DISCUSSION

Table II displays the data that have been obtained on the test set of Fig. 1, as well as experimentally observed specific rotations and results from previous TDDFT work based on the B3LYP hybrid functional.[17,18] The experimental values have been taken from the compilations in these references as well, except for **34** and **36**. Figure 2 graphically displays a comparison of the computational results with experimental data. Finally, Table III lists mean errors and median errors for the specific rotations calculated by the different methods as compared to experimental values (and therefore excluding **11** and **12**). The helicene data (**34**–**36**) have not been included in the mean and median values, but it can be seen from Table II that the quality of the results for the helicenes is comparable to what has been obtained for the other molecules. The same holds for **23**, the results of which are also not included in the arithmetic means of Table III due to the large magnitude of $[\alpha]_D$ and the resulting deterioration of the mean values.

From Fig. 2 as well as from Table III it becomes obvious that, independent of whether an LDA or GGA functional is used, basis set IV is not able to reproduce the experimental data with reasonable accuracy (except for the largest molecules in the test set). Large mean errors of approximately 100% and median errors of 40%–50% with large deviations, respectively, are obtained. The basis set Vd which contains both more polarization functions and additional diffuse functions performs significantly better here. Interestingly, the basis Vp which contains no diffuse functions but even more polarization functions than Vd performs comparably well, too (or even better than Vd). This might be taken as an indication that further improvement of the results could be obtained by extending the basis set Vd with the additional polarization functions of the Vp basis. The reason for the observed behavior lies in the fact that, in order to obtain an accurate description of both the $\boldsymbol{M}$ and the $\boldsymbol{D}$ integrals in Eq. (5) and also of the potential response to the electric and magnetic field, both additional polarization and diffuse functions are required.

The rather large differences between the mean and the median errors in Table III indicate that a few outlyers substantially contribute to the mean errors. Further, due to the large range of magnitudes of optical rotations and the large range of errors, referring to arithmetic mean or root mean square values is somewhat problematic here. For such situations, the median (in particular of the relative errors) is often better suited to describe the data. Upon inspection of Table II we find that particularly large systematic deviations between the calculated and the experimental $[\alpha]_D$ occur for **6**, **18**, and **19**. Note that for **18** an older but somewhat uncertain experimental $[\alpha]_D = 227°/(\mathrm{dm\,g/cm^3})$ has also been quoted in Refs. 18 and 8 which compares favorably with our other computations. Compound **6** appears to be a particularly difficult case for which all of our computations (and also all

TABLE III. Unsigned mean (Δ) and median (δ) errors of computed data with respect to experimental values[a] in deg/(dm g/cm^3), and the respective relative errors Δ^r and δ^r (last two columns, in %).

Method[b]	$\Delta[\alpha]_D$	$\Delta[\alpha]_D$[c]	$\delta[\alpha]_D$	$\Delta^r[\alpha]_D$[c]	$\delta^r[\alpha]_D$
LDA/IV	56±44	51±42	33±39	106±97	46±77
LDA/Vp	26±18	23±16	18±16	54±43	37±40
LDA/Vd	30±22	25±18	22±20	50±43	28±38
GGA/IV	49±41	43±37	28±35	93±89	41±71
GGA/Vp	26±20	19±13	16±18	45±36	34±36
GGA/Vd	31±24	24±16	18±21	47±37	30±37
SAOP/Vd	31±26	20±13	18±22	46±38	33±41
SIC/Vp	32±25	22±15	19±21	36±23	28±25
B3LYP	20±12	17±10	17±12	38±28	30±27

[a]Unsigned errors: arithmetic mean or median of $|[\alpha]_D^{\mathrm{calc.}} - [\alpha]_D^{\mathrm{expt}}|$ of the data of Table II excluding **11**, **12**, and **34–36**. **23** is also excluded from the arithmetic mean values. Unsigned mean deviations of mean and median errors indicated by "±." Relative errors: mean or median of $|[\alpha]_D^{\mathrm{calc.}} - [\alpha]_D^{\mathrm{expt}}|/|[\alpha]_D^{\mathrm{expt}}|$, in %.
[b]See Table II and Sec. III. B3LYP data from Refs. 17 and 18 (column II in Table II). For B3LYP, the first listed value of Table II has been used in case more than one value was available. SIC data does not contain **8** and **33**.
[c]Data set of footnote a excluding **6**, **18**, and **19**.

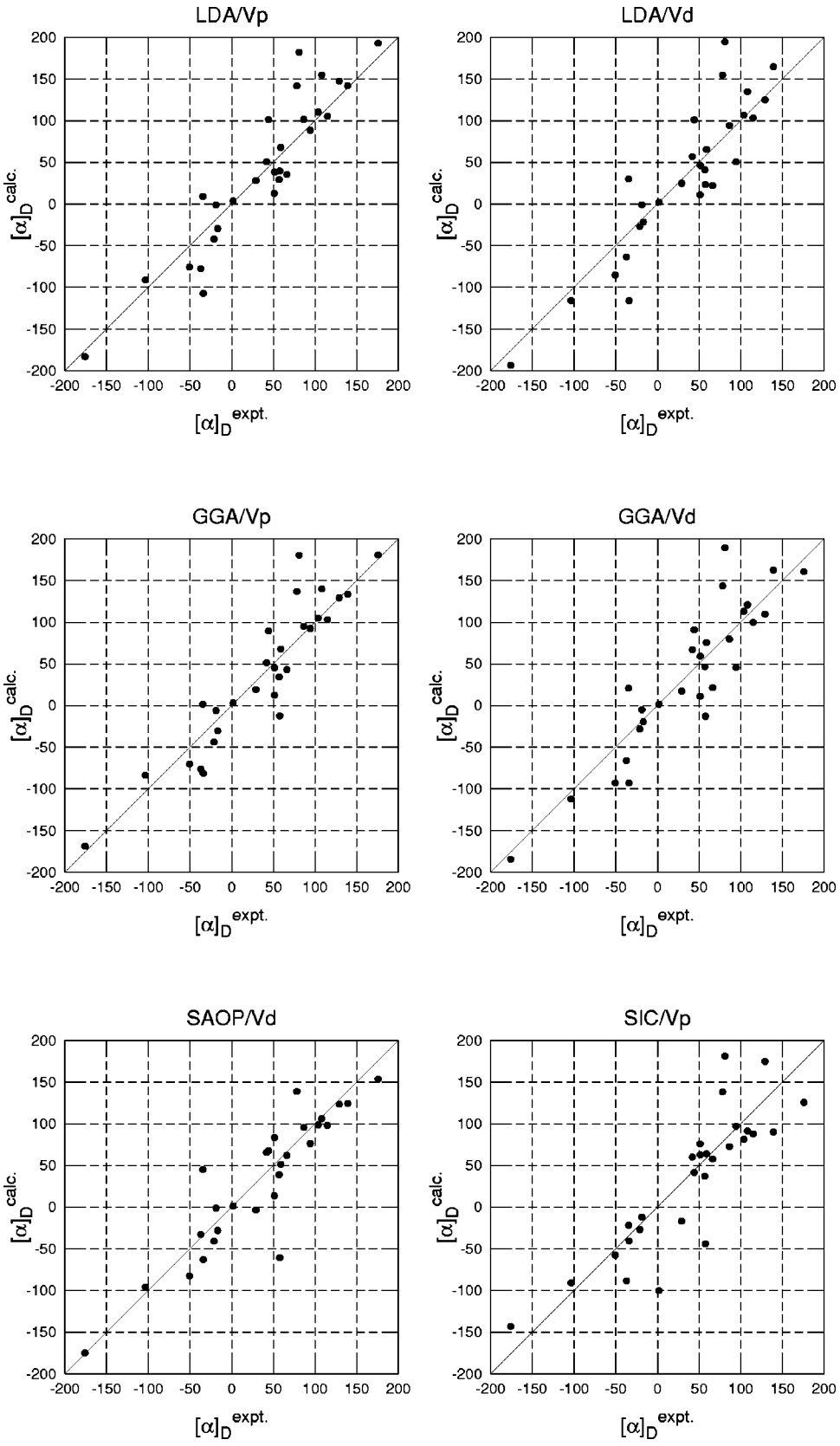

FIG. 2. Comparison of calculated specific rotations with experimental data in the range of $-200°$ to $200°/(\mathrm{dm\ g/cm^3})$, for the computations employing basis sets Vp and Vd.

other computations in Ref. 17 except the one that is quoted here) predict the wrong sign of $[\alpha]_D$. **19** has a very large optical rotation. Even though our calculations for **19** do not deviate more than about 30% from the experimental value, which is not an untypical value as compared to the rest of the test set, the magnitude of $[\alpha]_D$ contributes substantially to the mean errors. Excluding these three cases from the test set and reevaluating the mean errors results in a much better agreement between the mean and the median values. The final unsigned mean errors for the remaining 27 molecules

(25 for SIC/Vp) are quite comparable to the ones reported in Table 3 of Ref. 17 for the B3LYP functional with the aug-cc-pVDZ [20°/(dm g/cm^3)] and aug-cc-pVTZ [23°/(dm g/cm^3)] bases for almost the same test set (except of **6**, **15**, and **20**). Their calculations with the 6-311++G($2d$,$2p$) basis were reported to yield a best value of 19°/(dm g/cm^3) for the mean error. We have listed the results for the aug-cc-pVDZ basis of Ref. 17 in Table II in order to allow for an easier comparison with the results of Grimme[18] who also used (among other choices) the diffuse functions of the aug-cc-pVDZ basis for his computations. We have to stress here that the favorable comparison of the unsigned mean errors of the functionals being used here with the B3LYP data is dependent on whether a few outlyers are included or not included in the data set. Further, the deviation of the mean and median errors is significantly smaller in the case of B3LYP for the full data set. This means that the nonhybrid functionals being employed here are on average more likely to produce outlyers for this type of molecules. When optical rotations are only available from computations, it is probably reasonable to expect possible relative errors of up to 50%. Larger errors can be expected in case different density functionals yield largely deviating results.

Some cases in Table II that are worthwhile to point out here individually are **13** and **20**. For **13**, all nonhybrid methods except SIC yield the wrong sign for $[\alpha]_D$. SIC is here in very good agreement with the B3LYP results. On the other hand, SIC and also SAOP yield the wrong sign of the specific rotation in the case of **20**, where all other methods including B3LYP correctly predict sign and magnitude. Both molecules have rather small optical rotations. In all other cases, the signs and magnitudes of $[\alpha]_D$ obtained with the Vd and Vp basis sets are in agreement with experimental data and with the B3LYP results.

From the preceding discussion we conclude that nonhybrid functionals are on average almost as well suited to predict optical rotations of rigid organic molecules as the B3LYP hybrid functional, provided that high quality basis sets are employed. In comparison, Hartree–Fock calculations produce much larger mean errors [63°/(dm g/cm^3) with respect to experiment for the complete test set in Ref. 17] and significantly more outlyers. Based on the unsigned mean errors, neither SAOP nor SIC offer a large improvement of the LDA and GGA results. In both cases (compare Fig. 2) the good overall performance does not result in much smaller errors because of a few cases for which large deviations between theory and experiment remain. When comparing the relative errors (Table III), the SIC functional appears to perform best though (both mean and median). In this case, molecules with rather small specific rotations contribute a large amount to the relative errors [considering the overall mean deviations of 20°–30°/(dm g/cm^3)]. Most of these molecules are well described by SIC. Large deviations for some of the molecules with larger $[\alpha]_D$ at the same time cause unfavorable mean errors for this density functional. Previous experience with the SIC functional indicates that it is sometimes able to cure particularly "difficult cases" (such as, e.g., **13**), while it does only slightly influence the results for molecules that are already well described by standard LDA or GGA functionals. In the case of optical rotations here, SIC appears to perform somewhat less accurately than VWN and BP86 which is most likely due to drawbacks of its current implementation. As a result, the high SCF convergence that is required for an accurate determination of optical rotations is not always possible to achieve and the results are subject to larger numerical errors that the ones obtained with VWN or BP86 and the same basis set. This is true in particular for larger molecules or when many lone pairs are present in the molecule. With regard to the SAOP potential, it has been previously demonstrated that it improves in particular the energies for Rydberg excitations in small molecules. For valence excitations it does not yield much improved results as compared to standard GGA functionals. From the data in Table II it becomes obvious that in almost every case it influences the optical rotations significantly as compared to GGA/Vd, but on average (Table III) it does not offer a clear systematic improvement. Taking the size of the test set into account, the differences between the mean or median errors for SAOP/Vd and GGA/Vd or LDA/Vd are not very significant. We have previously noted that SAOP can improve individual rotatory strengths of low lying excitations for organic molecules.[14] At the same time, though, other examples that we have investigated did not show a clear improvement of the whole low-energy range of the CD spectrum in comparison with experiment, even though the excitation energies resulting from SAOP systematically agreed very well with the experimental ones. Therefore for these molecules we cannot necessarily expect an accurate prediction of the optical rotations by the SAOP potential.

It becomes clear from the data in Table III that at the present stage we cannot give a conclusive answer as to which of the density functionals (other than B3LYP) performs best for the computation of optical rotations, in particular since the results indicate that the basis sets can be further improved. It is well known that B3LYP performs well for many properties of organic molecules not containing heavy elements. We might expect a better performance of the pure density functionals for optical rotations of chiral transition metal complexes. A respective study by us is currently under way.

Regarding the frequency dependence of $\beta(\omega)$ we note that the specific rotation $[\alpha]_\omega$ for the zero frequency limit is zero, while β remains finite [see Eqs. (5) and (8)]. We do not make an attempt here to systematically compare "$[\alpha]_0$" values to experimental $[\alpha]_D$'s, where "$[\alpha]_0$" is obtained from $\beta(0)$ by applying the conversion factor for $\beta(D) \rightarrow [\alpha]_D$, since we regard this comparison not as physically meaningful. If both $\beta(\omega)$ and $\beta(0)$ yield a reasonable specific rotation by this procedure this means that both values are not much different, which is often the case. However, for some molecules one observes large variations of β, even in the low-frequency range. As an example, for heptahelicene $\beta(0) = -36.0$ a.u. and $\beta(D) = -81.2$ a.u. (GGA/IV) which would lead to an underestimation of the experimentally observed specific rotation by 41% (for "$[\alpha]_0$") or an overestimation by 34%. The average agreement with experimental data for the "$[\alpha]_0$" values for the complete test turns out not to be significantly different from the $[\alpha]_D$ values, when basis sets

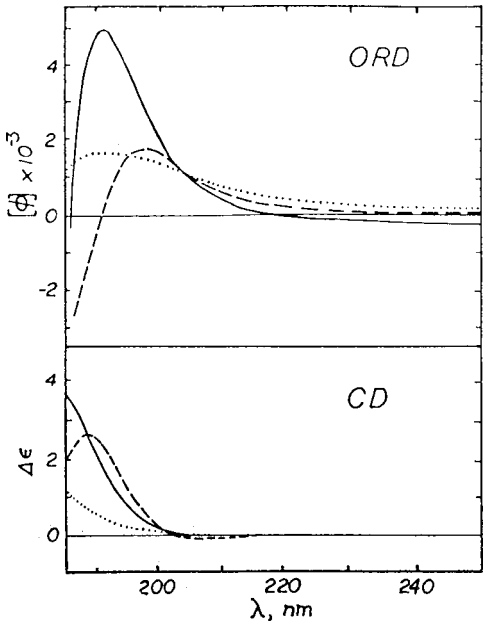

FIG. 3. Experimentally observed ORD and CD of compound **5** in the range of 180–250 nm (solid lines). The molecular rotation $[\phi]=[\alpha]\cdot M/100$ is shown instead of $[\alpha](\omega)$. Reprinted with permission from Ref. 46 © (1971) Americal Chemical Society.

Vp and Vd are employed. However, no meaningful ORD spectrum could be obtained from considering $\beta(0)$ alone, and the comparison with experimental data should systematically be based on the frequency dependent β's if available even if this leads to a less good agreement with experiment for individual cases. In order to demonstrate the usability of the present code for the prediction of ORD spectra, we have calculated the molecular rotation $[\phi]=[\alpha]\cdot M/100$ of compound **5** in the range of $\lambda=180-250$ nm. The experimental ORD and CD have been reported in Ref. 46 and are reprinted in Fig. 3. The calculated data (SAOP/Vd) are displayed in Fig. 4. It can be seen that the location of the electronic absorption around 185 nm and the resulting singularity and the sign change in the ORD spectrum are correctly reproduced by the computation. Due to the missing theoretical treatment of line shapes, the magnitude of the experimentally observed OR in the vicinity of the excitation wavelength cannot be

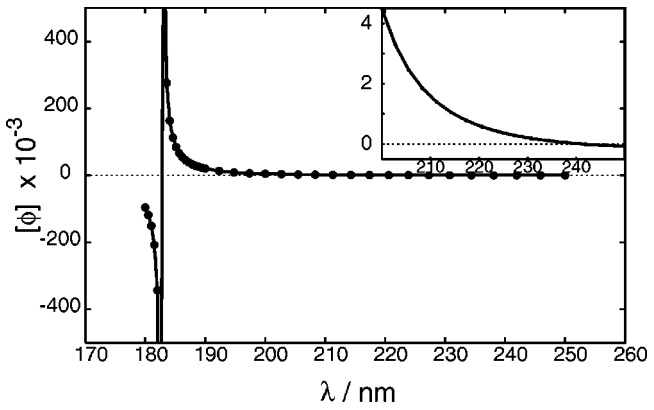

FIG. 4. Calculated ORD of compound **5** in the range of 180–250 nm (SAOP/Vd). See also Fig. 3.

expected to match the theoretical prediction. However, as shown in the inset of Fig. 4, not too close to the excitation wavelength the magnitude of the experimental $[\phi]$ agrees favorably with the computational data. Further, the sign change of the OR from negative to positive values when approaching the excitation wavelength from $\lambda>250$ nm is qualitatively well reproduced, though shifted to larger wavelengths in the simulated spectrum, Fig. 4. As has already been shown in Table II, the magnitude of the optical rotation at the *D* line wavelength agrees also rather well with the experimental value.

V. SUMMARY

We have implemented an extension to the RESPONSE module of the ADF program that makes it possible to calculate frequency dependent optical rotations based on TDDFT. A test set of 36 molecules has been investigated with different density functionals and basis sets. In comparison with experimental data it has been demonstrated that high quality basis sets need to be employed in order to obtain a reasonable accuracy.

The results obtained with the Vd and Vp basis sets suggest that some improvement could still be achieved by combining their flexibilities regarding polarization and diffuse functions. However, it is questionable if the agreement with experiment can be drastically improved by the use of more accurate density functionals and more flexible basis sets without taking the experimental conditions (solvents, temperature, ...) explicitly into consideration. Regarding the pure density functionals we cannot yet clearly identify a ''best'' functional as a zeroth order choice. Further improvements of the zeroth order functional in conjunction with more suitable basis sets will certainly have a positive influence on the results. For future developments, it can also be expected that going beyond the ALDA approximation for the XC kernel will improve optical rotations in cases where very high lying excitations yield significant contributions. Other factors that lead to a disagreement between the calculated and the experimental results have already been extensively discussed in the literature.[8,17,18] In particular for the molecules without a chromophor such as a π bond, the optical rotations are dominated by Rydberg excitations which in turn are subject to sizeable solvent effects. Apparently, the present density functional approach offers both a reasonable accuracy and error compensation in order to allow the prediction of optical rotations within the aforementioned range of errors without the need for modeling solvent effects. In fact, inclusion of solvent effects by simply considering the Lorentz factor of $(n^2+2)/3$ within the present approach reduces the agreement between theory and experiment.[17] Some other factors that can lead to a disagreement with experimental data are: (i) Errors in the optimized molecular geometries. Other authors have previously found[47] that for the simulation of CD spectra of certain rigid camphor derivatives, the results were only weakly influenced by the choice of different computational models for the geometry optimization (Hartree–Fock versus semiempirical PM3). However, other cases also involving rigid molecules have shown a strong sensitivity of rotatory strengths on small changes in the optimized geom-

etry, SCF convergence, etc.,[14] and we might consequently expect a pronounced sensitivity of optical rotations with respect to the molecular geometry in selected cases here as well. This is corroborated by the results of Ref. 17. (ii) Vibrational contributions have been neglected in the present work. (iii) Gauge dependency of the results. We have commented on this in Sec. III. (iv) Uncertainties in the experimental data. In some cases, the experimental rotations are extrapolated from data for not exactly known *ee*. Other uncertainties can arise from concentration effects.

The remaining difference between theoretical predictions and experimental data, based on a ''well behaved'' test set, is of the magnitude of $20°/(\mathrm{dm\,g/cm^3})$ for the Vd and Vp basis sets. The corresponding relative median errors are approximately 30%. This accuracy is valid for the specific type of systems being studied here: rather rigid organic molecules containing H, C, N, O, S, Cl (and F, Br in one case). For flexible molecules, a number of different conformers contribute to the experimental results and need consequently to be taken into account in the computational procedure. Further, it can be expected that the accuracy of TDDFT for optical rotations, and in particular the comparison with the B3LYP hybrid functional, will be much different when studying, e.g., chiral transition metal complexes.

ACKNOWLEDGMENT

This work has received financial support from the National Science and Engineering Research Council of Canada (NSERC).

[1] E. Charney, *The Molecular Basis of Optical Activity* (Wiley, New York, 1979).
[2] P. Crabbé, *Optical Rotatory Dispersion and Circular Dichroism in Organic Chemistry* (Holden-Day, San Francisco, 1965).
[3] *Circular Dichroism: Principles and Applications*, edited by K. Nakanishi, N. Berova, and R. W. Woody (VCH, New York, 1994).
[4] C. Djerassi, *Optical Rotatory Dispersion* (McGraw-Hill, New York, 1960).
[5] E. U. Condon, Rev. Mod. Phys. **9**, 432 (1937).
[6] A. Moscowitz, Adv. Chem. Phys. **4**, 67 (1962).
[7] A. E. Hansen and T. D. Bouman, Adv. Chem. Phys. **44**, 545 (1980).
[8] P. L. Polavarapu and D. K. Chakraborty, J. Am. Chem. Soc. **120**, 6160 (1998).
[9] E. K. U. Gross and W. Kohn, Adv. Quantum Chem. **21**, 255 (1990).
[10] E. K. U. Gross, J. F. Dobson, and M. Petersilka, Top. Curr. Chem. **181**, 81 (1996).
[11] J. F. Dobson, in *Electronic Density Functional Theory. Recent Progress and New Directions*, edited by J. F. Dobson, G. Vignale, and M. P. Das (Plenum, New York, 1998), pp. 43–53.
[12] F. Furche *et al.*, J. Am. Chem. Soc. **122**, 1717 (2000).
[13] R. Bauernschmitt and R. Ahlrichs, Chem. Phys. Lett. **256**, 454 (1996).
[14] J. Autschbach, T. Ziegler, S. J. A. van Gisbergen, and E. J. Baerends, J. Chem. Phys. **116**, 6930 (2002).
[15] J. R. Cheeseman, M. J. Frisch, F. J. Devlin, and P. J. Stephens, Chem. Phys. Lett. **252**, 211 (1996).
[16] F. J. Devlin, P. J. Stephens, J. R. Cheeseman, and M. J. Frisch, J. Am. Chem. Soc. **118**, 6327 (1996).
[17] P. J. Stephens, F. J. Devlin, J. R. Cheeseman, and M. J. Frisch, J. Phys. Chem. A **105**, 5356 (2001).
[18] S. Grimme, Chem. Phys. Lett. **339**, 380 (2001).
[19] K. Ruud and T. Helgaker, Chem. Phys. Lett. **352**, 533 (2002).
[20] K. Yabana and G. F. Bertsch, Phys. Rev. A **60**, 1271 (1999).
[21] Amsterdam Density Functional program, Theoretical Chemistry, Vrije Universiteit, Amsterdam, URL: http://www.scm.com
[22] G. te Velde and E. J. Baerends, J. Comput. Phys. **99**, 84 (1992).
[23] C. Fonseca Guerra, O. Visser, J. G. Snijders, G. te Velde, and E. J. Baerends, in *Methods and Techniques for Computational Chemistry* (STEF, Cagliari, 1995).
[24] G. te Velde *et al.*, J. Comput. Chem. **22**, 931 (2001).
[25] S. J. A. van Gisbergen, J. G. Snijders, and E. J. Baerends, J. Chem. Phys. **103**, 9347 (1995).
[26] S. J. A. van Gisbergen, J. G. Snijders, and E. J. Baerends, Comput. Phys. Commun. **118**, 119 (1999).
[27] P. R. T. Schipper, O. V. Gritsenko, S. J. A. van Gisbergen, and E. J. Baerends, J. Chem. Phys. **112**, 1344 (2000).
[28] S. Patchkovskii, J. Autschbach, and T. Ziegler, J. Chem. Phys. **115**, 26 (2001).
[29] J. Autschbach and T. Ziegler, J. Chem. Phys. **116**, 891 (2002).
[30] F. Furche, J. Chem. Phys. **114**, 5982 (2001).
[31] W. Kauzmann, *Quantum Chemistry* (Academic, New York, 1957).
[32] A. D. Buckingham, Adv. Chem. Phys. **12**, 107 (1967).
[33] C. Jamorski, M. E. Casida, and D. R. Salahub, J. Chem. Phys. **104**, 5134 (1996).
[34] M. E. Casida, in *Recent Advances in Density Functional Methods*, edited by D. P. Chong (World Scientific, Singapore, 1995), Vol. 1.
[35] P. Jørgensen and J. Simons, *Second Quantization-based Methods in Quantum Chemistry* (Academic, New York, 1981).
[36] S. J. A. van Gisbergen, C. Fonseca-Guerra, and E. J. Baerends, J. Comput. Chem. **21**, 1511 (2000).
[37] J. Guan *et al.*, J. Chem. Phys. **98**, 4753 (1993).
[38] S. J. A. van Gisbergen *et al.*, Phys. Rev. A **57**, 2556 (1998).
[39] D. P. Chong, S. J. A. van Gisbergen, and E. J. Baerends (unpublished).
[40] M. E. Casida, C. Jamorski, K. C. Casida, and D. R. Salahub, J. Chem. Phys. **108**, 4439 (1998).
[41] S. H. Vosko, L. Wilk, and M. Nusair, Can. J. Phys. **58**, 1200 (1989).
[42] A. D. Becke, Phys. Rev. A **38**, 3098 (1988).
[43] J. P. Perdew, Phys. Rev. B **33**, 8822 (1986).
[44] J. P. Perdew, Phys. Rev. B **34**, 7406 (1986).
[45] M. Carnell *et al.*, Chem. Phys. Lett. **180**, 477 (1991).
[46] W. R. Moore, H. W. Anderson, S. D. Clark, and T. M. Ozretich, J. Am. Chem. Soc. **93**, 4932 (1971).
[47] F. Pulm, J. Schramm, J. Hormes, S. Grimme, and S. Peyerimhoff, Chem. Phys. **224**, 143 (1997).
[48] H. J. Bestmann and W. Both, Chem. Ber. **107**, 2923 (1974).
[49] R. H. Martin, M. Flammang-Barbieux, J. P. Cosyn, and M. Gelbcke, Tetrahedron Lett. **31**, 3507 (1968).
[50] W. S. Brickell, A. Brown, C. M. Kemp, and S. F. Mason, J. Chem. Soc. A **1971**, 756.